

Universitat de Lleida

Document downloaded from:

<http://hdl.handle.net/10459.1/65005>

The final publication is available at:

<https://doi.org/10.1016/j.scitotenv.2017.11.316>

Copyright

cc-by-nc-nd, (c) Elsevier, 2017



Està subjecte a una llicència de [Reconeixement-NoComercial-SenseObraDerivada 4.0 de Creative Commons](https://creativecommons.org/licenses/by-nc-nd/4.0/)

1 **Polymer inclusion membrane to access Zn speciation: comparison with root uptake**

2 Ruben Vera^a, Clàudia Fontàs^a, Josep Galceran^b, Olga Serra^c, Enriqueta Anticó^{a*}

3 ^aChemistry Department, University of Girona, C/ Maria Aurèlia Capmany, 69, 17003
4 Girona, Spain.

5 ^bDepartament de Química. Universitat de Lleida and AGROTECNIO, Rovira Roure 191,
6 25198 Lleida, Spain

7 ^cLaboratori del Suro, Biology Department, C/ Maria Aurèlia Capmany, 69, 17003 Girona,
8 Spain.

9 * Corresponding author. Tel: +3497241; FAX: +3497241. E-mail:
10 enriqueta.antico@udg.edu

11

12 **Abstract**

13 Metal speciation studies can be performed with a new technique based on a functionalized
14 membrane. The estimation of not only the total amount of metal, but also the metal
15 available to living organisms is very important. In this context, we have investigated the
16 use of a polymer inclusion membrane (PIM) in a new tool for the determination of free
17 metal ion concentration. In order to check the usefulness of PIM devices in metal
18 speciation studies and metal availability to potato plants (*Solanum tuberosum*), Zn has
19 been chosen as a case study. The PIM designed for Zn transport uses polyvinyl chloride
20 (PVC) as polymer and di-(2-ethylhexyl) phosphoric acid (D2EHPA) as carrier, with
21 0.01M nitric acid in the receiving solution. The stability of the PIM has been
22 demonstrated and good linearity of PIM-device fluxes (J_{PIM}) with free metal
23 concentration was observed for total metal concentrations ranging from 3 μM up to 70
24 μM . The presence of different ligands, such as ethylenediaminetetraacetic acid (EDTA),
25 humic acid (HA) and citrate, greatly influences the measured J_{PIM} because the formation
26 of metal complexes in the donor phase decreases the free Zn concentration in the sample.
27 Good correlation has been found when comparing PIM fluxes and metal accumulation in
28 potato plants roots in the presence of EDTA. But, the root uptake did not change when
29 adding citrate and HA to the hydroponic medium, so the uptake does not always follows
30 the Free Ion Activity Model (FIAM). These ligands might induce physiological changes
31 in the roots and enhance metal uptake.

32 Keywords: Polymer inclusion membranes (PIMs); metal speciation; di-2-(ethylhexyl)
33 phosphoric acid (D2EHPA); zinc; roots.

34

35 **1 Introduction**

36 Dissolved trace metals in environmental water or in pore water of soils and sediments can
37 be found in numerous chemical forms or species, such as free ions, and inorganic or
38 organic complexes. Metal partitioning among the different forms is a dynamic process
39 that depends on different parameters such as type and concentration of ligands,
40 temperature, pH or redox conditions of the medium. It has been established that for
41 cationic metals, the concentration of the free, uncomplexed, metal ion is usually the best
42 predictor for both metal bioaccumulation and toxicity in most aquatic systems. This
43 general consensus has led to the predominance of the free ion activity model (FIAM),
44 which postulates that the metal uptake by an organism is proportional to the free ion
45 concentration of the metal in the surrounding solution. FIAM relies on the internalisation
46 flux being limiting, rather than the supply of the metal from the solution to the surface of
47 the organism (Wilkinson et al., 2004).

48 The biotic ligand model (BLM) is an extension of the FIAM taking into account the
49 competitive binding of cations and protons at the surface of the biological membrane (i.e.
50 the biotic ligand) (Di Toro et al., 2001). Despite being extensively accepted, exemptions
51 to these models have also been reported, and some studies point out that in the case of
52 higher plants, the uptake might be favoured by the presence of organic ligands, which
53 would facilitate the metal uptake at the roots (Gramlich et al., 2013; Samson and Visser,
54 1989; Wang et al., 2009). Indeed, apart from internalisation of the free cation (Zhao et al.,
55 2016; Degryse et al., 2006), other mechanisms can contribute to the uptake such as the
56 direct internalisation of intact metal complexes by the organism (simple diffusion across
57 the lipid bilayer or permeation across the lipid bilayer via a ligand transport site).

58 Different techniques have been developed to measure, not only metal speciation, but also
59 to estimate labile fractions available for organisms (Sierra et al., 2017; Jones et al., 2016).
60 This is the case of diffusive gradients in thin films (DGT) technique, for example,
61 consisting of a porous gel matrix attached to a layer of complexing cation exchange beads
62 (Chelex 100). DGT is nowadays widely accepted as a tool to monitor metal availability
63 and to calculate the so-called DGT concentrations (Davison, 2016; Davison and Zhang,
64 1994).

65 Permeation liquid membrane (PLM) techniques are used for the separation and
66 preconcentration of target elements, which are complexed by an organic complexing
67 agent supported in a membrane. This membrane separates two different aqueous
68 solutions: the donor (also called source or feed) phase, containing the sample with the
69 analyte, and the acceptor (also called receiving or stripping) phase, where the analyte is
70 accumulated. The transport is based on liquid-liquid extraction coupled with diffusion. In
71 the nineties, Buffle and Parthasarathy firstly reported PLM for speciation studies as an
72 approach to mimic the processes of metal transport across biological membranes
73 (Parthasarathy and Buffle, 1994). The metal flux across the membrane is evaluated from
74 the variation of the metal concentration in the acceptor solution as a function of time.
75 Under certain conditions, PLMs measure the free metal ion fraction (Pesavento et al.,
76 2009), and PLM has been used as a reliable sensor for free Ni concentrations down to 10^{-7}
77 M as reported by Bayen et al. (Bayen et al., 2007). Pb availability to freshwater algae
78 was studied by comparing PLM fluxes and Pb biouptake fluxes (Slaveykova et al., 2004).
79 Both, the simplicity of this technique and the large number of available complexing
80 agents render this methodology very attractive. However, a weak point is the poor
81 stability of the membrane due to the leaching of the organic extracting compound into the
82 aqueous adjacent phases (Buffle et al., 2000). This fact has seriously limited a wider use
83 of PLM.

84 In this work, we explore for the first time the use of a simple device based on a polymer
85 inclusion membrane (PIM) to determine free ion concentrations in aqueous samples (*i.e.*
86 specifically targeting one relevant fraction of the total concentration). The principles of
87 this system are similar to those of PLM, since the analyte is transported across the
88 membrane, by means of the carrier, from the donor to the acceptor phase. However, to
89 increase the stability of the membrane, this carrier is entrapped within a polymeric matrix,
90 normally made of cellulose triacetate (CTA) or polyvinyl chloride (PVC). The role of the
91 polymer is to provide mechanical strength to the membrane, and sometimes, besides these
92 components, the addition of a plasticizer is also necessary to improve the elasticity as
93 well as to modify the diffusion characteristics of the membrane (Almeida et al., 2012).
94 This improved stability, in addition to their easy preparation, low cost, versatility, good
95 chemical resistance and high efficiency, had led to the use of these membranes for
96 separation or preconcentration purposes of different metals or organic compounds
97 (Garcia-Rodríguez et al., 2015; Güell et al., 2011). PIMs made of PVC and the carrier di-

98 (2-ethylhexyl) phosphoric acid (D2EHPA) have been applied for the determination of the
99 time-weighted average total concentration of Zn (Almeida et al., 2014), but its use as
100 sensor for Zn speciation has - as far as we know- not been described yet. The
101 environmental relevance of this new sensor stems from the crucial role, as stated by FIAM
102 and BLM, of the free ion concentration on the ecotoxicological impact of the considered
103 element.

104 Zn is one of the essential trace metal micronutrients, required by plants in small amounts
105 for various biochemical reactions and physiological functions such as formation of
106 chlorophyll, photosynthesis and respiration (Humayan Kabir et al., 2014; Remans et al.,
107 2012). Even though Zn deficiency is more widespread than Zn toxicity, excessive Zn
108 accumulation affects the capacity to maintain homeostasis and can induce oxidative stress.
109 In this work, PIM fluxes for Zn in the absence and presence of organic ligands forming
110 complexes with different binding strength and charge, such as EDTA, citrate, and humic
111 acids, have been determined using as a donor phase a plant nutrient solution (*i.e.* a
112 hydroponic medium). Moreover, PIM fluxes have been compared with Zn uptake by
113 potato (*Solanum tuberosum*) roots under the same experimental conditions. Potato plants
114 were chosen for this study because (i) potato is the fifth largest staple crop consumed
115 worldwide, fulfilling essential needs in human nutrition and health (FAO, 2015), and (ii)
116 potato plantlets were reproduced asexually using cuttings, reducing the the overall
117 variability among samples and contributing to increase the reproducibility of the
118 experiment. Special attention is devoted to elucidate whether the the PIM-based sensor
119 (in the current conditions) are determining the free Zn concentration, rather than the total
120 concentration or any other fraction.

121

122 **2 Experimental**

123 **2.1 Reagents and solution**

124 All reagents and solvents used in this study were of analytical grade. The polymer PVC,
125 and the acid 2-(N-morpholino) ethanesulfonic (MES) were obtained from Fluka (Bern,
126 Switzerland). The organic solvent, tetrahydrofurane (THF), was purchased from Panreac
127 (Barcelona, Spain). The carrier, D2EHPA, was provided by Sigma-Aldrich (St Louis,
128 Missouri, USA). For the preparation of the hydroponic solution the following reagents,
129 purchased from Panreac (Barcelona, Spain), were used: ammonium nitrate (NH_4NO_3),
130 boric acid (H_3BO_3), calcium nitrate ($\text{Ca}(\text{NO}_3)_2 \cdot 4\text{H}_2\text{O}$), copper sulphate ($\text{CuSO}_4 \cdot 5\text{H}_2\text{O}$),

131 potassium nitrate (KNO_3), potassium dihydrogen phosphate (KH_2PO_4), sodium
 132 molybdate ($\text{Na}_2\text{MoO}_4 \cdot 2\text{H}_2\text{O}$), sodium hydroxide (NaOH), magnesium sulphate
 133 heptahydrate ($\text{MgSO}_4 \cdot 7\text{H}_2\text{O}$), potassium hydroxide (KOH), manganese chloride
 134 ($\text{MnCl}_2 \cdot 4\text{H}_2\text{O}$) and zinc sulphate seven hydrate ($\text{ZnSO}_4 \cdot 7\text{H}_2\text{O}$). As iron source the
 135 commercial product Kelamix Fe was used (Sicosa, Girona, Spain). Hoagland solution at
 136 half strength, used as a nutrient solution and donor medium, is described in Table 1. The
 137 pH of the solution was adjusted at 6.0 ± 0.1 using 2.5 mM MES. Suprapur grade nitric
 138 acid (HNO_3) was obtained from Panreac (Barcelona, Spain). Organic ligands such as L-
 139 histidine monohydrochloride monohydrate, humic acids sodium salt (HA, used as
 140 received), ethylenediaminetetraacetic acid (EDTA) were provided by Sigma-Aldrich (St
 141 Louis, Missouri, USA) and sodium citrate ($\text{Na}_3\text{C}_6\text{H}_5\text{O}_7 \cdot \text{H}_2\text{O}$) was obtained from Scharlau
 142 (Barcelona, Spain). Propidium iodide (PI) and Fluorescein di-acetate (FDA) stains were
 143 obtained from Sigma and Invitrogen (Thermo Fisher, Waltham, Massachusetts, USA).

144

145 Table 1. Chemical composition of the nutrient solution corresponding to a half-strength
 146 Hoagland solution, used as donor medium in all the experiments performed throughout
 147 the study.

Chemical compound	Concentration (μM)
KNO_3	2500
$\text{Ca}(\text{NO}_3)_2 \cdot 4\text{H}_2\text{O}$	2500
Fe (in Kelamix)	12
$\text{MgSO}_4 \cdot 7\text{H}_2\text{O}$	1000
NH_4NO_3	500
KH_2PO_4	250
MES	2500
H_3BO_3	23
$\text{MnCl}_2 \cdot 4\text{H}_2\text{O}$	4.57
$\text{ZnSO}_4 \cdot 7\text{H}_2\text{O}$	0.38
$\text{CuSO}_4 \cdot 5\text{H}_2\text{O}$	0.10
$\text{Na}_2\text{MoO}_4 \cdot 2\text{H}_2\text{O}$	0.25

148

149 Calibration standards of Zn were prepared using a 1000 mg L^{-1} stock solution for atomic
 150 spectroscopy (Sigma-Aldrich, St Louis, Missouri, USA). The working range was from

151 0.05 mg L⁻¹ to 2.5 mg L⁻¹ in the donor solution and 0.3 mg L⁻¹ to 15 mg L⁻¹ in 0.01M
152 nitric acid for the analysis of the receiving phase.

153 Ultrapure water from a MilliQ Plus water purification system (Millipore Ibérica S.A.,
154 Madrid, Spain) was used to prepare all solutions.

155

156 **2.2 Instrument and apparatus**

157 An Ethos Plus Milestone microwave with HPR-1000/10S high-pressure rotor and
158 temperature sensor (Sorisolet, Bergamo, Italy) was employed for acid digestion of samples.

159 A sequential inductively coupled plasma atomic emission spectrometer, ICP-OES,
160 (Liberty RL, Varian, Mulgrave, Vic., Australia) was used to determine the total
161 concentration of Zn ($\lambda = 213.81$ nm) in aqueous solutions and acid plant digestions. The
162 pH values of the aqueous samples were determined with a Crison Model GLP 22 pH
163 meter (Barcelona, Spain).

164 Fluorescent root plant images were obtained using an epifluorescence BX-41 Olympus
165 microscope that was connected to a DP-73 Olympus digital camera (Olympus, Tokyo,
166 Japan).

167

168 **2.3 Membrane preparation**

169

170 PIMs were prepared by dissolving 400 mg of PVC in 12 mL of THF and the resulting
171 mixture was stirred for 2 hours. Later on, the appropriate amount of carrier D2EHPA
172 (from a 0.5 M D2EHPA solution in THF) was added to the corresponding polymeric
173 solution and stirred again for 1 hour in order to obtain the final membrane composition
174 of 70% PVC-30% D2EHPA or 60% PVC-40% D2EHPA (% in mass). Finally, the
175 resulting mixture was poured out into a 9.0 cm diameter flat bottom glass petri dish, which
176 was set horizontally and covered loosely. The organic solvent was allowed to evaporate
177 during 24 h at room temperature, and the resulting film (of an approximate thickness of
178 55 μm) was afterward carefully peeled off from the bottom of the petri dish.
179 Reproducibility of the PIM preparation was routinely checked by means of total weight,
180 IR spectroscopy and thickness measurements.

181

182 **2.4 PIM-device experiments**

183 The designed device (see Fig. 1), with similarities to those previously reported (Almeida,
184 et al., 2014; Almeida et al., 2016) consists of a glass tube with two openings, one at the
185 top (0.9 cm diameter) and another one at the bottom (1.8 cm diameter). The PIM was
186 placed at the bottom opening (1.75 cm²) and fixed with a screw cap. The opening at the
187 top was closed with a standard screw cap and was used to fill the device with 5 mL of
188 receiving solution. To carry out the experiments using this device, 250 mL of donor
189 nutrient solution spiked with zinc (and organic ligands when indicated) were poured into
190 a glass beaker placed on a magnetic stirrer. The device incorporating the membrane and
191 receiving solution (5 mL 0.01M HNO₃) was immersed 1 cm in the donor nutrient solution
192 in a vertical position under stirring conditions. After the deployment period, the device
193 was removed from the solution and the receiving solution was taken for analysis. The
194 final concentration in the donor solution was also checked in order to verify that no
195 depletion took place.

196

197 Fig. 1

198 2.5 Plant growth

199 Potato plants (*Solanum tuberosum* cv Desireé) were grown *in vitro* in Murashige and
200 Skoog solid medium (MS) supplemented with 2% sucrose (Serra et al., 2008). 1-node
201 explants without leaves, using only axial gems of four week-old plants, were cultured *in*
202 *vitro* in solid MS for three weeks in order to ensure the homogeneity amongst the different
203 biological replicates. Then, they were transferred to the hydroponic media. Plants *in vitro*
204 and plants in hydroponics were grown under light/dark photoperiod cycle of 12/12 h at
205 67 μmol m⁻² s⁻¹ and 25 °C and 22 °C respectively

206

207 2.6 Plant exposure and analysis

208 Plant exposure to Zn and to the different organic ligands was studied following the
209 experimental design described in Fig. S1 (in the Supporting Information). From the *in*
210 *vitro* plants, fourteen plants (for each treatment) were grown in ten-litter buckets of
211 nutrient solution containing Hoagland's half strength solution (Table 1) during two weeks
212 before plant exposure to the metal or the ligand. The treatments include (i) no metal
213 addition (control experiment), (ii) fortified donor medium with 35 μM Zn (no ligand) and

214 (iii) three Zn-fortified media each with an added specific organic ligand at a final
215 concentration of 20 μM of EDTA, 240 μM citrate or 60 mg L^{-1} of HA. The ligand
216 concentrations for this study were selected so that, for a total Zn concentration of 35 μM ,
217 similar free Zn concentrations were reached in all treatments. Plants were exposed for a
218 period of 48 h. After that, plants were removed from buckets and carefully dipped into
219 cold water for 30 seconds prior to rinsing them with a 5 $\text{mM Pb}(\text{NO}_3)_2$ solution (Panreac,
220 Barcelona, Spain) to remove Zn from the surface of the roots. Finally, plants were dried
221 in an oven at 60°C for 5 days (Cuypers et al., 2002; Gramlich et al., 2013). Pools of roots
222 from 4 plants were cut into small pieces, dried and weighted before microwave acid
223 digestion. Then, they were transferred to PTFE vessels and digested with 8 mL of nitric
224 acid of suprapure grade (69%) and 2 mL of hydrogen peroxide (30%). The vessels were
225 closed and heated into the microwave following a digestion program consisting of a first
226 step of 5 min to reach 180 °C and then 10 min at 180 °C. After cooling, digested sample
227 solutions were transferred to a 30 mL flask and brought to volume with ultrapure de-
228 ionized water prior to ICP-OES analysis.

229

230 **2.7 Vital staining of roots**

231 Once the different exposures were finished, a pool of three plants were removed from the
232 buckets and their roots were cut and transferred directly to an aqueous solution containing
233 5 $\mu\text{g mL}^{-1}$ of PI and 2 $\mu\text{g mL}^{-1}$ of FDA for 15-30 min. The roots were then rinsed twice
234 with water, and mounted on a microscope slide which was subsequently submerged in
235 water (John et al., 1995). The samples were viewed within 15 min from the staining with
236 a BX-41 Olympus microscope that was connected to a DP-73 Olympus digital camera.
237 For FDA detection, we used the excitation filter B (excitation at 475 nm and emission at
238 515 nm using a long path filter). For PI detection, we used the excitation filter G
239 (excitation at 530 nm and emission at 610 nm). The same specimen was analysed
240 separately at wavelengths specific to each stain and the two images were merged to give
241 the final image.

242

243 **3 Results and discussion**

244

245 3.1 Evaluation of the PIM system

246 When speciation is of interest, the test sample composition should not be modified, and,
 247 in particular, the decrease in analyte concentration in the source solution due to membrane
 248 extraction should be negligible (*i.e.* no depletion of the analyte test sample). These
 249 conditions are usually achieved by using a volume of the test solution much larger than
 250 the volume of the acceptor phase, e.g. using a hollow fibre geometry (Tomaszewski et al.,
 251 2003; Slaveykova et al., 2009) or with "flow-through" approaches (Almeida et al., 2014).
 252 Apart from the donor and acceptor volumes, the membrane composition and the acceptor
 253 phase acidity can be modulated to ensure no depletion of the analyte in the donor phase.
 254 So, we fixed an aqueous volume of 250 mL for the donor solution and of 5 mL for the
 255 acceptor solution. We evaluated the effect on metal transport and depletion when the
 256 nutrient solution (without MES added) was supplemented with 35 μM Zn(II), and tested
 257 two nitric acid concentrations of 0.01 and 0.1 M in the acceptor phase and two PIM
 258 compositions. Results are presented in Table 2, in terms of metal concentration in both
 259 the donor and in the receiving solutions after 24 h experiment in each condition. As
 260 expected, the better the transport to the receiving solution (*i.e.* higher final concentrations
 261 in the acceptor), the larger the variation from the initial Zn concentration in the donor
 262 solution is obtained. Given that the use of a PIM made of 70% PVC- 30% D2EHPA and
 263 a 0.01 M HNO_3 receiving solution ensures the negligible depletion conditions required to
 264 perform our studies, we fixed these conditions for further experiments.

265

266 Table 2. Effect of PIM and receiving phase compositions on Zn transport and depletion.

267 Contact time: 24 h.

PIM	HNO_3 (M)	Initial [Zn] donor solution (μM)	Final [Zn] donor solution (μM)	[Zn] receiving solution (μM)
70% PVC- 30% D2EHPA	0.01	35.92	35.4	60.1
	0.1		31.6	120.7
60% PVC- 40% D2EHPA	0.01		30.1	131.7
	0.1		20.8	417.7

268

269 3.2 Stability studies

270 It has been extensively reported that the lack of stability is the main drawback of PLM
271 (Buffle et al., 2000). Gramlich et al. (2012) described the use of a PLM in hollow fibre
272 configuration consisting of a mixture of a Kryptofix 22DD and lauric acid as carriers
273 dissolved in phenylhexane and toluene (1:1 v/v) as solvents for the transport of free Zn.
274 They found a decrease in the transport capacity of the membrane down to 63 % within 8
275 h after impregnation. Therefore, it was necessary to use freshly impregnated membranes
276 in all experiments (which lasted 2 hours).

277 To study the stability of the PIM system, we evaluated the variation of Zn flux (J_{PIM} in
278 $\text{mol m}^{-2} \text{s}^{-1}$) with time. For that, three experiments were performed contacting the PIM-
279 devices with the corresponding donor solution and retrieved them at different times, from
280 24 to 48 h. The average flux can be calculated from the number of moles found in the
281 acceptor phase and considering the membrane area and the deployment time. Results are
282 collected in Fig. 2, where it can be seen that there is not a significant variation in Zn flux
283 for the time period studied, so one can assume the system to be under a steady-state
284 regime (Galceran and Puy, 2015). Moreover, the stability of the PIM was also evaluated
285 in terms of membrane mass loss, and it was found only a decline of $2.2 \pm 0.4\%$ of total
286 weight after 24 h of immersion (this corresponds to 7% carrier loss).

287 Fig. 2.

288 Hence, these results support the use of PIMs as an attractive alternative to PLM, since
289 they maintain the important features of PLMs such as simplicity, low cost and the
290 possibility to prepare selective membranes, while providing the necessary stability to
291 perform long-term experiments.

292 3.3 Measurement of diffusional J_{PIM}

293 Several experiments were performed to measure J_{PIM} in the absence of organic ligands.
294 The initial total metal concentration in the nutrient solution was varied from 3 μM up to
295 70 μM . J_{PIM} was calculated as before and, as can be seen in Fig. 3, it is proportional to
296 the free Zn^{2+} concentration in the donor phase (computed using visual MINTEQ with its
297 standard database, and neglecting the contribution of the complex Kelamix Fe (Yunta et
298 al., 2003)). The equation for a lineal model of J_{PIM} ($\text{nmol cm}^{-1} \text{h}^{-1}$) vs. $[\text{Zn}]$ (μM) is:

$$299 \quad J_{\text{PIM}} = 0.092(\pm 0.004) [\text{Zn}]_{\text{PIM}} - 0.27(\pm 0.15) \quad (1)$$

300 and $R^2 = 0.9905$

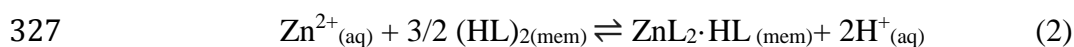
301 Fig. 3.

302 To test the real possibilities of PIM as a tool to measure the free ion concentrations,
303 different organic ligands have been used in this work: EDTA, citrate and humic acid.
304 EDTA is a polydentate ligand which forms strong complexes with metals and is used as
305 a ligand to buffer Zn^{2+} , as Zn-EDTA is assumed to barely contribute to Zn uptake (Bell
306 et al., 2003; Hart et al., 1998; Stacey et al., 2008). Citrate is involved in the storage of Zn
307 in plant vacuoles (White et al., 2009). Finally, humic acid is a part of the natural organic
308 matter which plays an important role in aquatic ecosystems by binding trace metals and,
309 thus, influencing their speciation, bioavailability, and toxic effects. Thus, 20 μM of
310 EDTA, 60 $mg L^{-1}$ of HA or 240 μM of citrate were added to the growth medium. J_{PIM}
311 was evaluated in the presence of these ligands at two different total metal concentrations,
312 35 and 70 μM . We could observe that the addition of organic ligands produced a decrease
313 in all J_{PIM} , which correlates with the reduction of free Zn according to visual MINTEQ
314 calculations. $[Zn^{2+}]_{PIM}$ was determined (using the calibration provided by Fig. 3 and
315 plotted in Fig. 4 together with $[Zn^{2+}]_{MINTEQ}$ and the 1:1 line on which both values should
316 match. The good agreement found supports the claim that the sensor is measuring free Zn
317 concentrations. Moreover, the use of PIMs as a new speciation technique (as an
318 alternative to PLM) appears as a promising possibility.

319 Fig. 4.

320 3.4 Modelling the flux of Zn

321 Separation by means of functionalized membranes is based on the chemical affinity of
322 the target compound towards the ligand or functional group existing inside the membrane.
323 In both, PLMs and PIMs, an appropriate carrier is added to the membrane to interact with
324 the analyte, Zn^{2+} in this study. For this work, the extraction reaction of the metal by
325 D2EHPA (denoted as HL) can be described with the following equilibrium reaction
326 (Kolev et al., 2009):



328

329 Taking into account our current data and similarly to existing literature on PLM (Buffle
330 et al., 2000), a simple model can be derived from the following hypotheses:

331 A) equilibrium at both interfaces.

332 For the Donor/membrane (indicated as superscript D/m) interface

$$333 \quad K = \frac{[\text{ZnL}_2 \cdot \text{HL}]^{\text{D/m}} \left([\text{H}^+]^{\text{D/m}} \right)^2}{\left([(\text{HL})_2]^{\text{D/m}} \right)^{3/2} [\text{Zn}^{2+}]^{\text{D/m}}} \quad (3)$$

334 while for the membrane/Acceptor (indicated as superscript m/A) interface

$$335 \quad K = \frac{[\text{ZnL}_2 \cdot \text{HL}]^{\text{m/A}} \left([\text{H}^+]^{\text{m/A}} \right)^2}{\left([(\text{HL})_2]^{\text{m/A}} \right)^{3/2} [\text{Zn}^{2+}]^{\text{m/A}}} \quad (4)$$

336 All concentrations in these section are expressed in mol m⁻³.

337

338 B) diffusion co-limitation of the fluxes, both in the membrane

$$339 \quad J^{\text{m}} = \frac{D_{\text{ZnL}_2 \cdot \text{HL}}^{\text{m}}}{\ell} \left([\text{ZnL}_2 \cdot \text{HL}]^{\text{D/m}} - [\text{ZnL}_2 \cdot \text{HL}]^{\text{m/A}} \right) \quad (5)$$

340 (where ℓ is the thickness of the membrane, in m, and $D_{\text{ZnL}_2 \cdot \text{HL}}^{\text{m}}$ is the diffusion
341 coefficient, in m² s⁻¹, of the complexed carrier inside the membrane) and in the Acceptor
342 solution

$$343 \quad J^{\text{A}} = \frac{D_{\text{Zn}^{2+}}}{\delta^{\text{A}}} \left([\text{Zn}^{2+}]^{\text{m/A}} - 0 \right) \quad (6)$$

344 (where δ^{A} is the thickness of the diffusion layer in the Acceptor and $D_{\text{Zn}^{2+}}$ is the
345 diffusion coefficient of free Zn ion there).

346 C) Given that the presence of labile ligands (see Fig 4) does not relevantly increase J_{PIM}
347 (but rather J_{PIM} is proportional to the free Zn concentration), we assume that there is no
348 limitation by diffusion in the Donor solution

$$349 \quad [\text{Zn}^{2+}]^{\text{D/m}} \approx [\text{Zn}^{2+}]^* \quad (7)$$

350 where superscript * indicate the bulk concentration of the sample. This also leads to

$$351 \quad [\text{H}^+]^{\text{D/m}} \approx [\text{H}^+]^* \quad (8)$$

352

353 D) Steady state is assumed taking into account the lack of variation of J_{PIM} seen in Fig 2.354 In steady-state regime, all fluxes of Zn (be it complexed or free) have to be equal to the
355 resulting flux

$$356 \quad J^{\text{m}} = J^{\text{A}} = J_{\text{PIM}} \quad (9)$$

357

358 Simple algebra using previous assumptions leads to

$$359 \quad J_{\text{PIM}} = \frac{K \left([(\text{HL})_2]^{\text{D/m}} \right)^{3/2}}{\left([\text{H}^+]^* \right)^2} [\text{Zn}^{2+}]^* \quad (10)$$

$$\frac{\ell}{D_{\text{ZnL}_2 \cdot \text{HL}}^{\text{m}}} + \frac{K \left([(\text{HL})_2]^{\text{m/A}} \right)^{3/2}}{\left([\text{H}^+]^{\text{m/A}} \right)^2} \frac{D_{\text{Zn}^{2+}}^{\text{A}}}{\delta^{\text{A}}}$$

360

361 In general, $[(\text{HL})_2]^{\text{D/m}}$ and $[(\text{HL})_2]^{\text{m/A}}$ are not constant, but depend on the loading of
362 Zn, because of the balance of ligand, e.g. at interface Donor/membrane,

$$363 \quad 2 \times [(\text{HL})_2]^{\text{D/m}} + 3 \times [\text{ZnL}_2 \cdot \text{HL}]^{\text{D/m}} = c_{\text{T,L}} \quad (11)$$

364 where $c_{\text{T,L}}$ stands for the total D2EHPA (monomer) concentration inside the membrane.

365

366 Given the observed linear relationship between flux and free concentrations, we consider
367 “excess of ligand” conditions, i.e. the amount of Zn bound to the carrier is approximately
368 constant:

$$369 \quad [(\text{HL})_2]^{\text{D/m}} \approx \frac{c_{\text{T,L}}}{2} \approx [(\text{HL})_2]^{\text{m/A}} \quad (12)$$

370

371 Considering the fast diffusion of protons and their huge concentration (in comparison to
372 Zn)-, one can take

373 $[\text{H}^+]^{m/A} \approx [\text{H}^+]^A$

374

375 With these considerations, eqn (10) simplifies to

376
$$J_{\text{PIM}} \approx \frac{\frac{K(c_{\text{T,L}}/2)^{3/2}}{([\text{H}^+]^*)^2} [\text{Zn}^{2+}]^*}{\frac{\ell}{D_{\text{ZnL}_2\cdot\text{HL}}^m} + \frac{K(c_{\text{T,L}}/2)^{3/2} D_{\text{Zn}^{2+}}^A}{([\text{H}^+]^A)^2 \delta^A}} \quad (13)$$

377

378 This expression justifies:

379 i) the linearity of the steady-state flux with free Zn concentration (Figs. 3 and 4) and the
 380 lack of impact of labile complexes present in the donor solution. This proportionality is
 381 reflected in eqn.(1), where the non-null intercept can be attributed to experimental
 382 uncertainty as well as to the system having an initial transient regime not considered in
 383 eqn. (13);

384 ii) higher fluxes when the acceptor is more acidic, *i.e.* higher $[\text{H}^+]^A$ (in Table 2, for
 385 instance, in the case of 30% D2EHPA, compare the final accumulated $[\text{Zn}^{2+}]$ in the
 386 acceptor around 121 μM for 0.1 M HNO_3 with $[\text{Zn}^{2+}]$ around 60 μM for 0.01 M HNO_3)

387 and iii) higher fluxes are expected for higher total carrier concentrations, *i.e.* higher $c_{\text{T,L}}$
 388 (in Table 2, for instance, in the case of 0.01 M HNO_3 , compare the final accumulated
 389 $[\text{Zn}^{2+}]$ around 132 μM for 40% D2EHPA with $[\text{Zn}]$ around 60 μM for 30% D2EHPA)

390

391 Apart from limitation by diffusion in both the membrane and in the acceptor solutions (as
 392 underlying eqn (13)), the accumulation rate of the analyte might be affected by other
 393 processes such as interfacial kinetics (which could become critical for low concentrations
 394 of carrier), but this is not considered here given some previous reported results with PIM
 395 (Fontàs et al., 2007; Kolev et al., 2013) and given that the model agrees with our current
 396 data.

397

398 Further experiments varying the membrane thickness and the carrier ligand concentration
399 over a range of values (Van Leeuwen et al., 2005), can confirm or discard the present
400 model and experimentally tune the PIM to probe the free fraction or others (such a labile
401 one).

402

403 **3.5 Toxicity of the ligands for the roots**

404 According to the FIAM paradigm, biological fluxes are directly proportional to free metal
405 ion concentrations rather than to the total ones (Campbell, 1995). This assumption has
406 been tested using living organisms such as freshwater algae (Bayen et al., 2006;
407 Slaveykova et al., 2004), microalgae (Rodríguez-Morales et al., 2015) or wheat plants in
408 hydroponics media (Gramlich et al., 2014). Alternatively, fluxes measured with the
409 different speciation techniques (PLM, DGT) have also been correlated with metal
410 bioavailability in some systems (Bradac et al., 2009). However, it is essential to take into
411 account the intrinsic metal and ligand toxicity before biological fluxes are measured. It
412 has been described that metal chelates at higher concentrations may damage roots, which
413 in turn affects metal uptake (Bell et al., 2003).

414 So, we performed viability analyses of the roots of potato plants growing in the different
415 donor solution media with 35 μM Zn and supplemented with the different ligands.
416 Distinction between viable and inviable cells was performed through a double fluorescent
417 staining procedure. FDA is cleaved by esterases present in living cells and fluoresces
418 green after it is cleaved. On the other hand, PI fluoresces red in the nuclei of dead cells.
419 PI also stains most of the cell walls, viable or inviable, which means that PI staining
420 sometimes overlaps FDA staining and appears yellow. In potato plants, young lateral
421 roots are viable when no treatment is applied (Fig. 5 a) and all the root tips assessed
422 presented green colour. When 35 μM metal content was supplemented in the donor
423 solution, roots succeeded in being stained with FDA and a green colour was obtained in
424 root tips (Fig. 5 b). Likewise, in treatments where 35 μM metal content and either EDTA,
425 HA or citrate were applied as ligands, cells were metabolically active and thus, green
426 colour was also predominant (Fig. 5 c-e). Lateral roots treated with the same amount of
427 Zn and histidine ligand, failed to stain with FDA, but were stained with PI (red),
428 suggesting that the cells die as a consequence of the treatment (see Fig. 5 f). Therefore,
429 measurements with histidine as a ligand were not reported in previous section 3.3, and
430 also not considered in what follows.

431 Fig. 5.

432 **3.6 Plant metal uptake and comparison with J_{PIM}**

433 Predicting availability of metals to plants is a challenge that has been addressed using
434 different approaches. For example, in the case of soil fertility evaluation and risk
435 assessment of soil contaminants, diethylenetriaminepentaacetic acid (DTPA)-extracts and
436 CaCl_2 (0.01 M) extractable concentrations are commonly used (Lindsay and Norvell,
437 1978; Meers et al., 2007; Menzies et al., 2007). Moreover, models based on a mechanistic
438 approach have been employed to describe uptake of major nutrients and micro-nutrients,
439 such as Mn and Zn (Adhikari and Rattan, 2000; Sadana and Claassen, 2000). Additionally,
440 DGT and PLM techniques have been suggested as tools to predict metal bioavailability
441 and different studies have been reported. The limiting transport steps in PLMs and
442 biological plasma membranes have been compared (Buffle et al., 2000; Degryse et al.,
443 2009). Despite being the transport processes in the test solution almost identical for living
444 organisms and PLM setup, the size and geometry of the systems clearly differ. Also,
445 relevant differences may arise in the transport steps at the water-membrane interface or
446 inside the membrane, despite being conceptually similar processes: the nature of the
447 binding sites is different, multistep processes usually account for the transport in
448 biological membranes, and passive diffusion of lipophilic complexes is differently
449 affected by the viscosity and other physical parameters. In any case, PLM has been used
450 to test the FIAM model, and considering the advantages of PIMs compared to PLM, we
451 have performed a series of experiments devoted to compare J_{PIM} with fluxes in plant roots.
452 Thus, the accumulated Zn in the roots was measured and "normalized" fluxes (J_{root}) were
453 computed by using the dry weight of the roots instead of an area. Zn normalized fluxes
454 obtained were in the range $0.56 \pm 0.05 - 1.10 \pm 0.05 \text{ nmol mg}^{-1} \text{ h}^{-1}$. A control experiment
455 with no Zn supplementation, showed also some metal uptake ($0.12 \pm 0.02 \text{ nmol mg}^{-1} \text{ h}^{-1}$)
456 due to the presence of just a trace amount of Zn in the donor solution.

457 The normalized biological fluxes are shown in figure 6 for the different treatments. An
458 ANOVA test was performed and significant differences ($p = 0.05$) were found among the
459 treatments. As can be seen, in the treatment with EDTA, the obtained root plant uptake
460 was lower compared to the treatment without ligand, which supports that the total
461 concentration of Zn in the solution is not the best indicator for uptake. This tendency can
462 also be observed in Fig. S2 (Supporting Information), where normalized J_{root} -values are
463 represented in front of J_{PIM} .

464 In the presence of humic acid and citrate, the found root fluxes are practically identical to
465 the fluxes without ligand. Similar results for citrate were found by other authors
466 (Gramlich et al., 2013) and were attributed to the high lability and mobility of these metal-
467 organic complexes that dissociate in the vicinity of the root surface. The direct uptake of
468 undissociated complexes has also been reported. In these situations, FIAM would not
469 apply (i.e. the uptake is not proportional to the free concentration).

470 In the case of HA, we have observed the formation of lateral roots (Fig. S3 in the
471 Supporting Information), which in turn would increase the exchange area and would yield
472 a metal uptake higher than expected. Moreover, the adsorption of humic substances into
473 biological surfaces can increase their negative surface charge and, thus, enhance their
474 overall electrostatic attraction for cations (Zhao et al., 2016). The increase of cell
475 permeability in the presence of humic acids can contribute to metal internalization as
476 described in (Slaveykova et al., 2003; Vigneault et al., 2000; Samson and Visser, 1989).
477 For higher plants as spinach or wheat, deviations from the FIAM have repeatedly been
478 reported (Degryse et al., 2009; Gramlich et al., 2013) pointing out that metal uptake in
479 roots is highly dependent on many factors, such as the plant species, metal concentration
480 and the rate of dissociation of metal complexes, among others.

481 Fig. 6.

482 **4 Conclusions**

483 In this study we have developed a simple technique based on a polymer inclusion
484 membrane to assess Zn speciation in a complex nutrient solution. The stability of this type
485 of membrane is substantially improved, rendering this technique suitable for (relatively)
486 long speciation experiments. When a PIM made of 70% CTA and 30% D2EHPA is
487 incorporated in a special device and a 0.01 M HNO₃ solution is used as an acceptor phase,
488 a correlation is found with the free metal, both in absence and in presence of ligands (EDTA,
489 citrate and humic acids). This correlation is the basis for PIM to determine [Zn²⁺] and has
490 been justified with a model consistent with existent evidences. We have also evidenced the
491 need to consider viability and physiological changes of the roots prior to study metal
492 internalization. Additionally, when comparing J_{PIM} and metal uptake by potato plant roots,
493 different behaviours arise depending on the ligand. In the case of Zn-citrate and Zn-HA
494 complexes we have observed a direct proportionality between total metal and root uptake.
495 However, in the case of EDTA, this relationship is observed for free metal.

496

497 **Acknowledgments**

498 The financial support of the Spanish government through research projects CTM2013-
499 48967 and CTM2016-78798(AEI/FEDER/UE) is acknowledged. R.Vera acknowledges a
500 grant from Spanish Ministerio de Economía y Competitividad ref. BES-2014-068314.

501

502 **References**

- 503 Adhikari T, Rattan RK. Modelling zinc uptake by rice crop using a Barber-Cushman
504 approach. *Plant Soil* 2000; 227:235–42.
- 505 Almeida MIGS, Cattrall RW, Kolev SD. Recent trends in extraction and transport of
506 metal ions using polymer inclusion membranes (PIMs). *J Memb Sci* 2012;415–
507 416:9–23.
- 508 Almeida MIGS, Chan C, Pettigrove VJ, Cattrall RW, Kolev SD. Development of a
509 passive sampler for Zinc(II) in urban pond waters using a polymer inclusion
510 membrane. *Environ Pollut* 2014;193:233–9.
- 511 Almeida MIGS, Silva AML, Coleman RA, Pettigrove VJ, Cattrall RW, Kolev SD.
512 Development of a passive sampler based on a polymer inclusion membrane for total
513 ammonia monitoring in freshwaters. *Anal Bioanal Chem* 2016;408:3213–22.
- 514 Bayen S, Wilkinson KJ, Buffle J. The permeation liquid membrane as a sensor for free
515 nickel in aqueous samples. *Analyst* 2007;132:262–7.
- 516 Bayen S, Worms I, Parthasarathy N, Wilkinson K, Buffle J. Cadmium bioavailability and
517 speciation using the permeation liquid membrane. *Anal Chim Acta* 2006;575:267–
518 73.
- 519 Bell PF, Mclaughlin MJ, Cozens G, Stevens DP, Owens G, South H. Plant uptake of 14
520 C-EDTA, 14C-Citrate, and 14C-Histidine from chelator-buffered and conventional
521 hydroponic solutions. *Plant Soil* 2003;253:311–319.
- 522 Bradac P, Behra R, Sigg L. Accumulation of Cadmium in Periphyton under Various
523 Freshwater Speciation Conditions. *Environ Sci Technol* 2009;43:7291–96.
- 524 Buffle J, Parthasarathy N, Djane L, Matthiasson L. Permeation liquid membranes for field
525 analysis and speciation of trace compounds in waters. In: Buffle J, Hoarvai G, editors.
526 In Situ Monitoring of Aquatic Systems; Chemical Analysis and Speciation. West
527 Sussex, (UK): John Wiley & Sons; 2000. p. 407–93.
- 528 Campbell PGC. Interactions between trace metals and aquatic organisms: a critique of
529 the free-ion activity model. In: Tessier A., Turner D, editors. Metal speciation and
530 bioavailability in aquatic systems, vol.3. Chichester (UK): John Wiley & Sons; 1995.

- 531 p. 45–102 (IUPAC series on analytical and physical chemistry of environmental
532 systems, Chapter 2).
- 533 Cuyppers, ANN, Vangronsveld J, Clijsters H. Peroxidases in roots and primary leaves of
534 *Phaseolus vulgaris* Copper and Zinc Phytotoxicity: a comparison. *J Plant Physiol*
535 2002;159:869–76.
- 536 Davison W, editor. *Diffusive Gradients in Thin-Films for Environmental Measurements*,
537 Cambridge Environmental Chemistry Series. Cambridge (UK): Cambridge
538 University Press; 2016.
- 539 Davison W, Zhang H. In situ speciation measurements of trace components in natural
540 waters using thin-film gels. *Nature* 1994;367:546–8.
- 541 Degryse F, Smolders E, Parker DR. Metal complexes increase uptake of Zn and Cu by
542 plants: implications for uptake and deficiency studies in chelator-buffered solutions.
543 *Plant Soil* 2006;289:171–85.
- 544 Degryse F, Smolders E, Zhang H, Davison W. Predicting availability of mineral elements
545 to plants with the DGT technique: A review of experimental data and interpretation
546 by modelling. *Environ Chem* 2009;6:198–218.
- 547 Di Toro DM, Allen HE, Bergman HL, Meyer JS, Paquin PR, Santore RC. Biotic ligand
548 model of the acute toxicity of metals. 1. Technical basis. *Environ Toxicol Chem*
549 2001;20:2383–96.
- 550 Fontàs C, Tayeb R, Dhahbi M, Gaudichet E, Thominet F, Roy P, Steenkeste K,
551 Fontaine-Aupart MP, Tingry S, Tronel-Peyroz E, Seta P. Polymer inclusion
552 membranes: The concept of fixed sites membrane revised. *J Memb Sci* 2007;290:
553 62–72.
- 554 Galceran J, Puy J. Interpretation of diffusion gradients in thin films (DGT) measurements:
555 a systematic approach. *Environ Chem* 2015;12:112–22.
- 556 Garcia-Rodríguez A, Matamoros V, Kolev SD, Fontàs C. Development of a polymer
557 inclusion membrane (PIM) for the preconcentration of antibiotics in environmental
558 water samples. *J Memb Sci* 2015;492:32–9.
- 559 Gramlich A, Tandy S, Frossard E, Eikenberg J, Schulin R. Diffusion limitation of zinc

- 560 fluxes into wheat roots, PLM and DGT devices in the presence of organic ligands.
561 *Environ Chem* 2014;11:41–50.
- 562 Gramlich A, Tandy S, Frossard E, Eikenberg J, Schulin R. Availability of zinc and the
563 ligands citrate and histidine to wheat: Does uptake of entire complexes play a role?
564 *J Agric Food Chem* 2013;61:10409–17.
- 565 Gramlich A, Tandy S, Slaveykova VI, Duffner A, Schulin R. The use of permeation liquid
566 membranes for free zinc measurements in aqueous solution. *Environ Chem*
567 2012;9:429–37.
- 568 Güell R, Anticó E, Kolev SD, Benavente J, Salvadó V, Fontàs C. Development and
569 characterization of polymer inclusion membranes for the separation and speciation
570 of inorganic As species. *J Memb Sci* 2011;383:88–95.
- 571 Hart J, Norvell W, Welch R, Sullivan L, Kochian L. Characterization of zinc uptake,
572 binding, and translocation in intact seedlings of bread and durum wheat cultivars.
573 *Plant Physiol* 1998;118:219–26.
- 574 Humayan Kabir A, Swaraz AM, Stangoulis J. Zinc-deficiency resistance and
575 biofortification in plants. *J Plant Nutr Soil Sci* 2014;177:311–19.
- 576 John LC, Grisafi PL, Fink GR. A pathway for lateral root formation in *Arabidopsis*
577 *thaliana*. *Genes & Dev* 1995;9:2131–42.
- 578 Jones AM, Xue Y, Kinsela AS, Wilchen KM, Collins RN. Donnan membrane speciation
579 of Al, Fe, trace metals and REE in coastal lowland acid sulfate soil-impacted
580 drainage waters. *Sci Total Environ* 2016;547:104–13.
- 581 Kolev SD, Baba Y, Cattrall RW, Tasaki T, Pereira N, Perera JM, Stevens GW. Solid
582 phase extraction of zinc (II) using a PVC-based polymer inclusion membrane with
583 di (2-ethylhexyl) phosphoric acid (D2EHPA) as the carrier. *Talanta* 2009;78:795–9.
- 584 Kolev SD, St John AM, Cattrall RW. Mathematical modeling of the extraction of
585 uranium(VI) into a polymer inclusion membrane composed of PVC and di-(2-
586 ethylhexyl) phosphoric acid. *J Memb Sci* 2013;425–426:169–75.
- 587 Lindsay WL, Norvell WA. Development of a DTPA Soil Test for Zinc, Iron, Manganese,
588 and Copper. *Soil Sci Soc Am J* 1978;42:421–8.

- 589 Meers E, Samson R, Tack FMG, Ruttens A, Vandegehuchte M, Vangronsveld J, Verloo,
590 MG. Phytoavailability assessment of heavy metals in soils by single extractions and
591 accumulation by *Phaseolus vulgaris*. *Environ Exp Bot* 2007;60: 385–96.
- 592 Menzies NW, Donn MJ, Kopittke PM. Evaluation of extractants for estimation of the
593 phytoavailable trace metals in soils. *Environ Pollut* 2007;145:121–30.
- 594 Parthasarathy N, Buffle J. Capabilities of supported liquid membranes for metal
595 speciation in natural waters: application to copper speciation. *Anal Chim Acta*
596 1994;284:649–59.
- 597 Pesavento M, Alberti G, Biesuz R. Analytical methods for determination of free metal
598 ion concentration, labile species fraction and metal complexation capacity of
599 environmental waters: A review. *Anal Chim Acta* 2009;631:129–41.
- 600 Remans T, Opdenakker K, Guisez Y, Carleer R, Schat H, Vangronsveld J, Cuypers A.
601 Exposure of *Arabidopsis thaliana* to excess Zn reveals a Zn-specific oxidative stress
602 signature. *Environ Exp Bot* 2012;84:61–71.
- 603 Rodríguez-Morales EA, De San Miguel ER, De Gyves J. Evaluation of the measurement
604 of Cu(II) bioavailability in complex aqueous media using a hollow-fiber supported
605 liquid membrane device (HFSLM) and two microalgae species (*Pseudokirchneriella*
606 *subcapitata* and *Scenedesmus acutus*). *Environ Pollut* 2015; 206:712–19.
- 607 Sadana US, Claassen N. Manganese dynamics in the rhizosphere and Mn uptake by
608 different crops evaluated by a mechanistic model. *Plant Soil* 2000;218:233–8.
- 609 Samson G, Visser SA. Surface-active effects of humic acids on potato cell membrane
610 properties. *Soil Biol Biochem* 1989;21:343–7.
- 611 Serra O, Soler M, Hohn C, Sauveplane V, Pinot F, Franke R, Schreiber L, Prat S, Molinas
612 M, Figueras M. CYP86A33-Targeted Gene Silencing in Potato Tuber Alters Suberin
613 Composition, Distorts Suberin Lamellae, and Impairs the Periderm's Water Barrier
614 Function. *Plant Physiol* 2008;149:1050–60.
- 615 Sierra J, Roig N, Giménez Papiol G, Pérez-Gallego E, Schumacher M. Prediction of the
616 bioavailability of potentially toxic elements in freshwaters. Comparison between
617 speciation models and passive samplers. *Sci Total Environ* 2017;605-606:211–8.

- 618 Slaveykova VI, Karadjova IB, Karadjov M, Tsalev DL. Trace Metal Speciation and
619 Bioavailability in Surface Waters Trace Metal Speciation and Bioavailability in
620 Surface Waters of the Black Sea Coastal Area Evaluated by HF-PLM and DGT.
621 Environ Sci Technol 2009;43:1798–803.
- 622 Slaveykova VI, Parthasarathy N, Buffle J, Wilkinson KJ. Permeation liquid membrane
623 as a tool for monitoring bioavailable Pb in natural waters. Sci Total Environ
624 2004;328:55–68.
- 625 Slaveykova VI, Wilkinson KJ, Ceresa A, Pretsch E. Role of fulvic acid on lead
626 bioaccumulation by *Chlorella kesslerii*. Environ Sci Technol 2003;37:1114–21.
- 627 Stacey SP, McLaughlin MJ, Çakmak I, Hettiarachchi GM, Scheckel KG, Karkkainen M.
628 Root Uptake of Lipophilic Zinc - Rhamnolipid Complexes. J Agric Food Chem
629 2008;56:2112–7.
- 630 Tomaszewski L, Buffle J, Galceran J. Theoretical and Analytical Characterization of a
631 Flow-Through Permeation Liquid Membrane with Controlled Flux for Metal
632 Speciation Measurements. Anal Chem 2003;75:893-900.
- 633 Van Leeuwen HP, Town R, Buffle J, Cleven R, Davison W, Puy J, Van Riemsdijk W,
634 Sigg L. Dynamic speciation analysis and bioavailability of metals in aquatic systems.
635 Environ Sci Technol 2005;39:8545–56.
- 636 Vigneault B, Percot A, Lafleur M, Campbell PGC. Permeability changes in model and
637 phytoplankton membranes in the presence of aquatic humic substances. Environ. Sci.
638 Technol. 2000;34:3907–13.
- 639 Wang P, Zhou DM, Luo XS, Li LZ. Effects of Zn-complexes on zinc uptake by wheat
640 (*Triticum aestivum*) roots: A comprehensive consideration of physical, chemical and
641 biological processes on biouptake. Plant Soil 2009;316:177–92.
- 642 White PJ, White PJ, Broadley MR. Biofortification of crops with seven mineral elements
643 often lacking in human diets- iron, zinc, copper, calcium, magnesium, selenium and
644 iodine. New Phytol 2009;182:49–84.
- 645 Wilkinson KJ, Buffle J. Critical evaluation of physicochemical parameters and processes
646 for modelling the biological uptake of trace metals in environmental (aquatic)

647 systems. Van Leeuwen HP, Köster W, editors. In *Physicochemical Kinetics and*
648 *Transport at Biointerfaces*. Chichester (UK) John Wiley & Sons; 2004. p. 447-533.

649 Yunta F, García-Marco S, Lucena JJ, Gómez-Gallego, M, Alcázar R, Sierra MA.
650 Chelating agents related to ethylenediamine bis(2-hydroxyphenyl)acetic acid
651 (EDDHA): Synthesis, characterization, and equilibrium studies of the free ligands
652 and their Mg²⁺, Ca²⁺, Cu²⁺, Fe³⁺ chelates. *Inorg. Chem.* 2003;42:5412–21.

653 Zhao CM, Campbell PGC, Wilkinson KJ. When are metal complexes bioavailable?
654 *Environ. Chem.* 2016;13:425–33.

655

656

657

658

659

660

661

662

663

664

665

666

667

668

669 **Figure captions**

670 Fig 1. Schematics of the PIM device and the whole setup used in the experiments

671 Fig 2. Evolution of PIM flux in front of the device deployment time. The initial
672 concentration was 35 μM of Zn. The values show the mean \pm SD ($n = 2$).

673 Fig 3. J_{PIM} at different free Zn concentrations in the donor phase added to the half-strength
674 Hoagland medium. PIM deployment time was 24 h. The values show the mean \pm SD
675 ($n=3$).

676 Fig 4. Comparison of $[\text{Zn}^{2+}]$ determined with the PIM device and the free concentration
677 calculated with MINTEQ for several source solutions consisting of half strength
678 Hoagland medium without and with added ligands (EDTA, HA and citrate). Deployment
679 time was 48 h. Full symbols, 70 μM total Zn; empty symbols, 35 μM total Zn. The values
680 show the mean \pm SD ($n=3$). The solid line is the 1:1 along which $[\text{Zn}^{2+}]_{\text{MINTEQ}}$ would
681 exactly match $[\text{Zn}^{2+}]_{\text{PIM}}$.

682 Fig 5. Representative epifluorescent micrographs of roots stained with FDA (green
683 nuclei) showing the living cells and PI (red nuclei) showing the dead cells after different
684 treatments: control with no Zn added (a) and 35 μM of Zn content (b) supplemented with
685 20 μM EDTA (c), 60 mg L^{-1} of HA (d), 240 μM citrate (e) and 20 μM of histidine(f).

686 Fig 6. Comparison of normalized root fluxes (35 μM Zn treatment and supplemented with
687 EDTA, HA and citrate as ligands). Deployment time was 48 h. The values show the mean
688 \pm SD ($n = 3$).

689